

55

## PHOTOELECTRON BRANCHING RATIOS AND ASYMMETRY PARAMETERS OF THE TWO OUTERMOST MOLECULAR ORBITALS OF METHYL CYANIDE

D.M.P. HOLLAND

*Institute of Physical Science and Technology, University of Maryland, College Park,  
MD 20742 (U.S.A.)*

A.C. PARR

*Synchrotron Ultraviolet Radiation Facility, National Bureau of Standards, Washington,  
DC 20234 (U.S.A.)*

J.L. DEHMER

*Argonne National Laboratory, Argonne, IL 60439 (U.S.A.)*

(First received 28 August 1983; in final form 20 January 1984)

### ABSTRACT

Vibrationally resolved photoelectron branching ratios and asymmetry parameters have been determined for the two outermost molecular orbitals of methyl cyanide. The results are discussed briefly within the context of similar studies on cyanogen and hydrogen cyanide, and in relation to structures exhibited in the photoionization efficiency curve.

### INTRODUCTION

In the last few years, there have been significant advances towards a deeper understanding of molecular photoionization. The key to much of this progress lies in the successful interaction between experiment and theory. Recent triply differential photoelectron studies — differential in incident photon wavelength, photoelectron kinetic energy, and photoelectron ejection angle — have provided the detailed information needed to assess which of the various theoretical models [1] give an adequate description of molecular photoionization dynamics. On the theoretical side, aid has been given in interpreting the experimental data, and in defining the mechanisms responsible for the observed effects.

Recently, there has been considerable interest in studying the way in which the photoionization process is affected by resonance phenomena (see, for example, refs. 2 and 3 and references therein). The early success in studying shape resonance phenomena both experimentally [4-6], and theoretically [7, 8], in nitrogen has influenced much of the subsequent work on such effects, and has led to extensive investigations being carried out on the first row diatomics. In particular, molecules have been chosen that possess a bond similar to the nitrogen  $N\equiv N$  bond. Accordingly, the cyanide group with a  $C\equiv N$  bond has attracted some attention. We have performed triply differential photoelectron studies on three cyanides: cyanogen [9], hydrogen cyanide [10] and methyl cyanide, in order to investigate the effect of placing the  $C\equiv N$  group in different chemical environments. Here we present the results for methyl cyanide,  $CH_3CN$ .

In a recent study on methyl cyanide using photoionization mass spectrometry, Rider et al. [11] have reported the photoionization efficiency curves for the parent and various daughter ions from threshold to approximately 20 eV. Earlier investigations [12-14] using the same technique gave values for the first ionization potential only. Electron impact energy-loss spectroscopy [15, 16] has enabled analysis of the Rydberg series converging to the ground and the first excited states of the ion. Photoelectron spectroscopy at 21.2 eV [17-20], 40.8 eV [21], and in the X-ray region [22, 23] has been used to determine the valence and inner valence ionization thresholds. Theoretical studies [24-26] on  $CH_3CN$  (acetonitrile) are in agreement with experimental observations in predicting that the molecular orbital sequence in its electronic ground state ( $C_{3v}$  symmetry) may be written as

$$(1a_1)^2(2a_1)^2(3a_1)^2(4a_1)^2(5a_1)^2(6a_1)^2(1e)^4(7a_1)^2(2e)^4$$

The two lowest ionization potentials are well established and may be given as [11, 27]:  $(2e)^{-1} X^2E = 12.194$  eV, and  $(7a_1)^{-1} A^2A_1 = 13.133$  eV. The next two ionization potentials, which fall within the photon energy range covered in the present experiment, are not well known and the experimental values show a considerable variation. The best values seem to be  $(1e)^{-1} B^2E = 15.13$  eV [19] and  $(6a_1)^{-1} C^2A_1 = 17.4$  eV [21].

## EXPERIMENTAL

The experiment was performed using a hemispherical electron analyzer [28] coupled to a 2 m normal incidence monochromator [29] connected to the SURF-II storage ring at the National Bureau of Standards. The experimental technique and method of data analysis have been described previously [30]. The spectrograde methyl cyanide sample was obtained from the Eastman Kodak Company and was thoroughly degassed by repeated

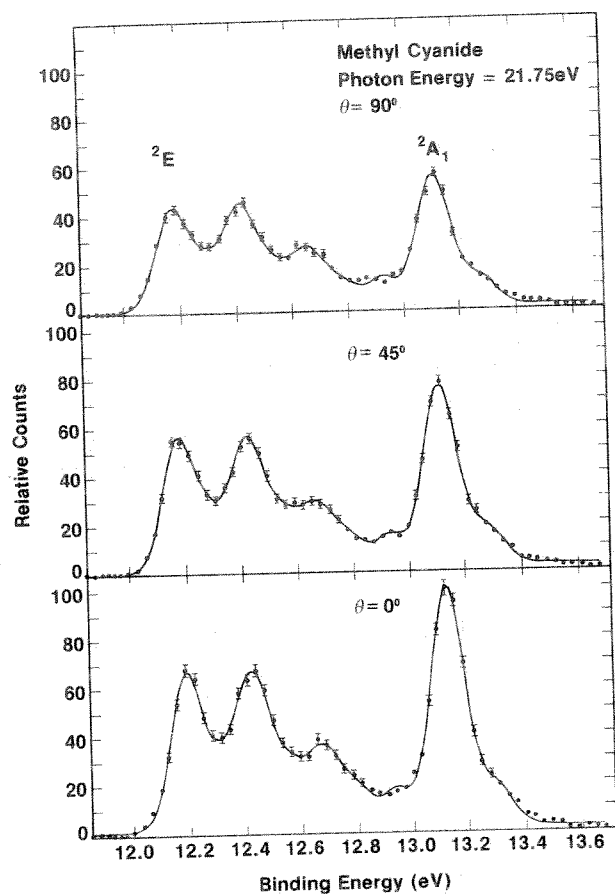


Fig. 1. Photoelectron spectra of methyl cyanide at photon energy 21.75 eV and at  $\theta = 0^\circ$ ,  $45^\circ$  and  $90^\circ$ . The spectra are normalized so that the maximum count in the  $\theta = 0^\circ$  spectrum equals 100. The data points ( $\bullet$ ) and the nonlinear least squares fit curve (—) are indicated.

freeze-pump-thaw cycles. A typical set of data, together with the result of a least-squares fit to Gaussian lineshapes, is shown in Fig. 1. Under the conditions appertaining to the present experiment, the differential cross section in the dipole approximation may be written as

$$\frac{d\sigma}{d\Omega} = \frac{\sigma_{\text{total}}}{4\pi} \left[ 1 + \frac{\beta}{4} (3P \cos 2\theta + 1) \right] \quad (1)$$

where  $\beta$  is the photoelectron asymmetry parameter,  $\theta$  is the photoelectron ejection angle relative to the major polarization axis, and  $P$  is the polarization of the incoming radiation. Equation (1) was used to deduce the asymmetry parameters and branching ratios presented in Fig. 2-8.

## RESULTS AND DISCUSSION

The experimental data were analyzed by incorporating the vibrational energies from Turner et al. [19] into a Gaussian fitting routine. Turner et al. observed the excitation of three vibrational modes in the ionic ground state, and assigned these as  $\nu_2$ , C $\equiv$ N stretching;  $\nu_3$ , symmetrical CH<sub>3</sub> deformation; and  $\nu_4$ , C—C stretching. The vibrational energies were 0.249, 0.177 and 0.100 eV respectively. In analyzing the present data for the X-state band, three vibrational progressions were used, and will be denoted as I, II, and III. Series I: a progression in  $\nu_2$ , with  $v_2$  taking values 0, 1, 2, 3;  $v_1 = 0$ ,  $v_3 = 0$ ,  $v_4 = 0$ . Series II: a progression in  $\nu_2$ , with  $v_2$  taking values 0, 1, 2;  $v_1 = 0$ ,  $v_3 = 1$ ,  $v_4 = 0$ . Series III: a progression in  $\nu_2$ , with  $v_2$  taking values 0, 1;  $v_1 = 0$ ,  $v_3 = 0$ ,  $v_4 = 1$ . Hence, all three series are progressions in  $\nu_2$ , with Series II and III having additional single excitations in  $\nu_3$  and  $\nu_4$  respectively.

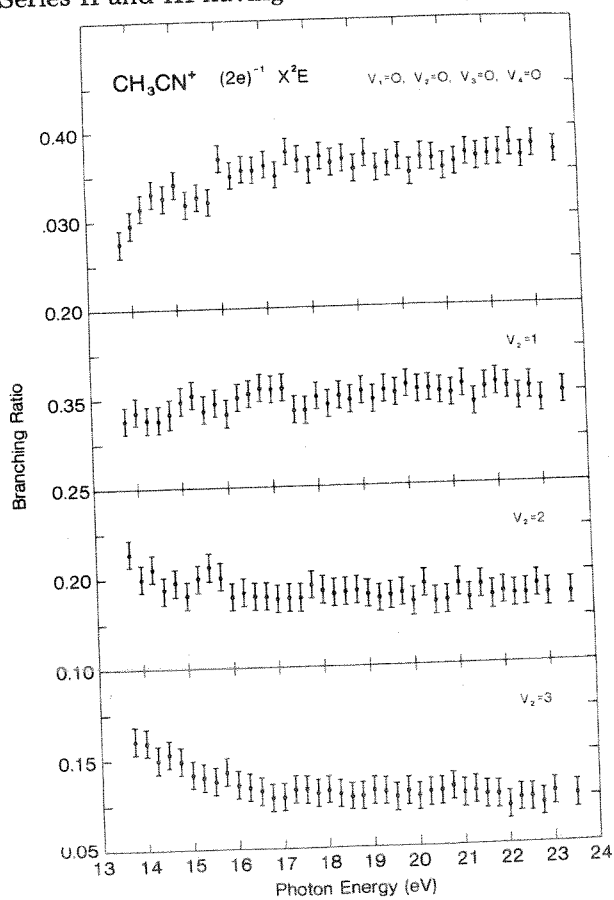


Fig. 2 Vibrational branching ratios for Series I ( $v_1 = 0$ ;  $v_2 = 0, 1, 2, 3$ ;  $v_3 = 0$ ;  $v_4 = 0$ ) of the X state.

This interpretation is identical to that proposed by Turner et al., apart from Series III, in which they managed to observe the  $v_2 = 2$  member. The A-state band, which can be attributed to photoionization of one of the nitrogen lone pair electrons, consists of a simple progression in  $\nu_3$ , with the first two members being observed.

A further note of clarification regarding the fitting procedure is warranted. The use of the nine Gaussians in Series I, II, and III to fit the poorly resolved X state in Fig. 1 was reluctantly adopted, after observing that this set of levels gave the best quality-of-fit for the overall spectrum and for the strong Series I. For instance, removing Series III noticeably degraded the fit of Series I and II and of the total spectrum. We therefore chose to analyze and present the data in this way, although the results for the weaker Series III should be recognized as less reliable than those for the stronger series.

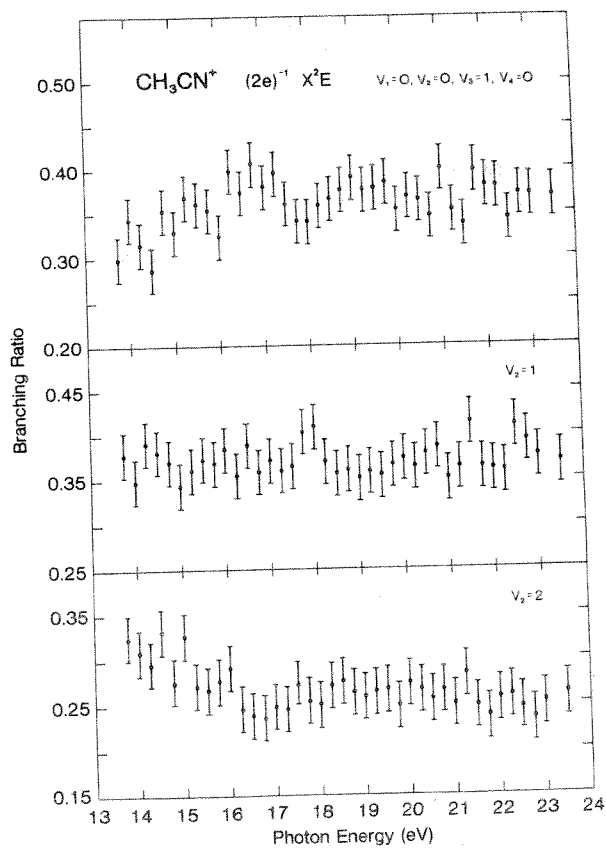


Fig. 3. Vibrational branching ratios for Series II ( $v_1 = 0; v_2 = 0, 1, 2; v_3 = 1; v_4 = 0$ ) of the X state.

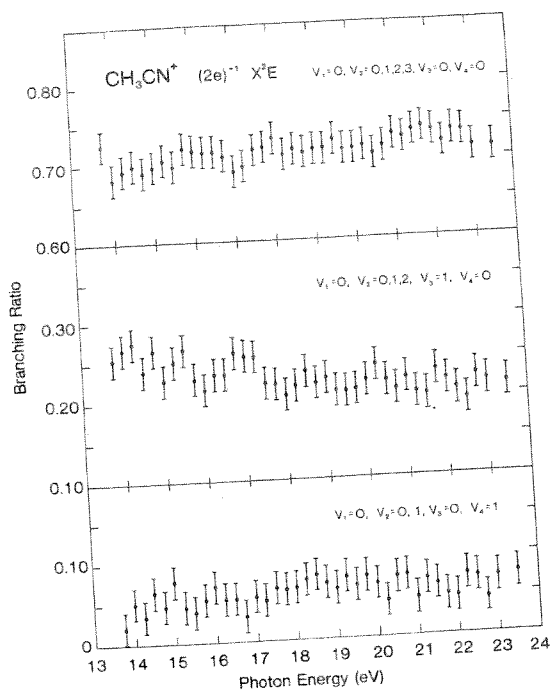


Fig. 4. Branching ratios for the total intensities in Series I, II and III of the X state.

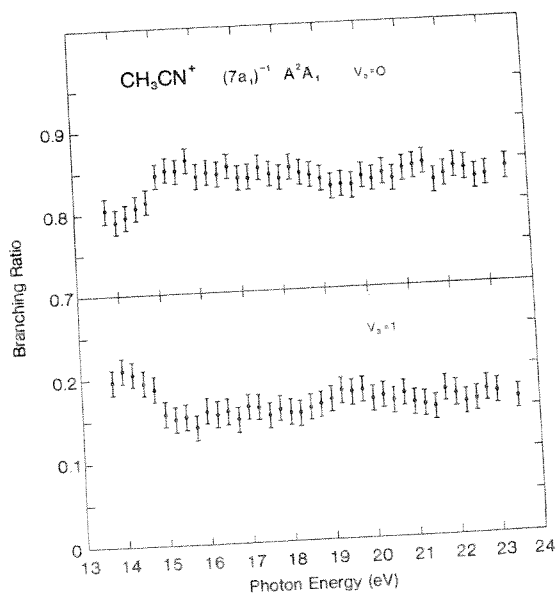


Fig. 5. Vibrational branching ratios of the A state.

The vibrational branching ratios of the  $X$  and the  $A$  states are shown in Figs. 2–5. Figures 2 and 3 illustrate the spectral variation in the vibrational branching ratios for the two major progressions of the  $X$  state, that is, Series I and II. Figure 4 shows the total intensities in the three separate vibrational progressions, Series I, II, and III, belonging to the  $X$  band. Although it is difficult to make a precise comparison with the single photoelectron spectrum obtained by Turner et al., it would appear that the two sets of experimental data indicate similar total contributions from the three series. In Fig. 5 the  $A$ -state vibrational branching ratio is displayed, and Fig. 6 shows the electronic branching ratio between the  $X$  and  $A$  states. The spectral variations in the vibrationally resolved asymmetry parameters for Series I of the ground ionic state are shown in Fig. 7a, b and c, and the vibrationally averaged asymmetry parameter for the entire  $X$  state is shown in Fig. 7d. Figure 8 displays the  $A$ -state vibrationally resolved asymmetry parameter.

In the photon energy region between the  $A$ - and  $B$ -state thresholds, that is, approximately 13–15 eV, the parent-ion photoionization efficiency curve is dominated by a single intense broad peak. Rider et al. [11] attributed this feature to autoionization, as it falls within a Franck–Condon gap of the photoelectron spectrum. Between 14.2 and 15.4 eV, weak Rydberg structure converging to the  $B$  state threshold is superimposed upon this peak. The vibrationally resolved branching ratios for Series I and II of the  $X$  state, (Figs. 2 and 3) and for the  $A$  state (Fig. 5) show weak energy-dependent variations from threshold to about 16 eV. At higher energies the branching ratios remain approximately constant. These weak deviations from the Franck–Condon values coincide with the energy region spanned by the broad peak in

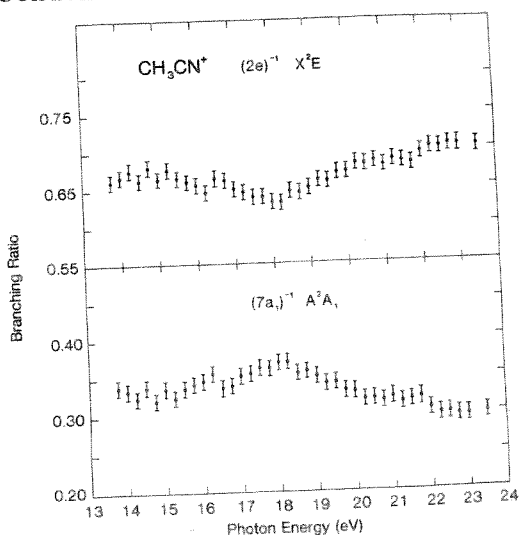


Fig. 6. Electronic branching ratios for the  $X$  and  $A$  states.

the photoionization efficiency curve. It is known [3] that autoionization can produce energy dependent effects in vibrational branching ratios. The theoretical work of Bieri et al. [26] predicts that the  $8a_1$  and the  $3e$  virtual orbitals lie between 4 and 5 eV in the continuum. Both of these orbitals have dipole allowed transitions from orbitals of  $a_1$  or  $e$  symmetry. Hence, it is not inconceivable that, by allowing a slight shift in the calculated energy levels, an intravalence transition could account for the broad peak in the photoionization efficiency curve and for the energy-dependent branching ratios observed in the present experiment.

Another mechanism which has been shown to influence the photoionization dynamics of small molecules is shape resonance phenomena.

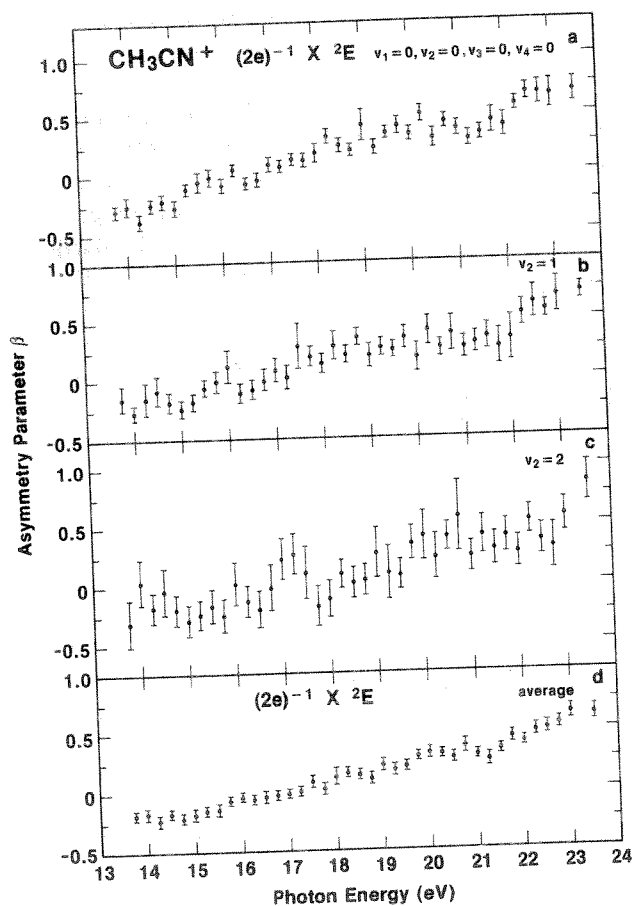


Fig. 7. a, b and c: Vibrationally resolved asymmetry parameter for series I ( $v_1 = 0; v_2 = 0, 1, 2; v_3 = 0; v_4 = 0$ ) of the X state. d, Vibrationally averaged asymmetry parameter of the X state.

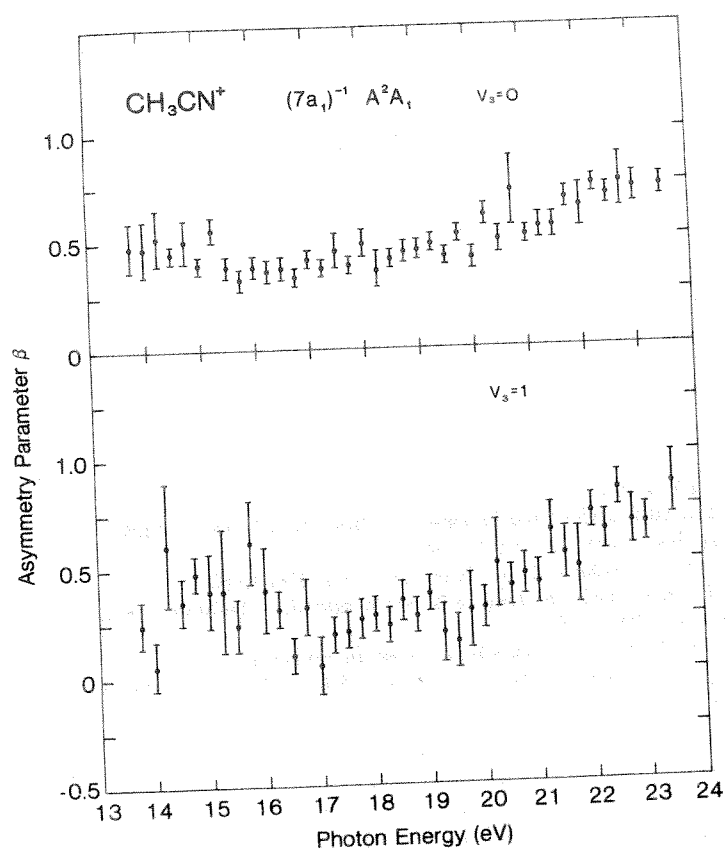


Fig. 8. Vibrationally resolved asymmetry parameter of the A state.

However, in similar studies performed on cyanogen [9] and hydrogen cyanide [10] it was suggested that shape resonant effects associated with the  $\text{C}\equiv\text{N}$  bond would not play a role until photon energies above those covered in the present experiment. It is reasonable to expect that this also applies to the present case of methyl cyanide. Unfortunately,  $K$  shell spectra, which would help clarify this situation, are not available. Hence, it seems prudent to save further comments on this matter until theoretical work has been performed to investigate the possible influence of resonant effects upon the photoionization dynamics of methyl cyanide.

#### ACKNOWLEDGMENTS

We thank R.P. Madden for his support and encouragement throughout this work. We appreciate the valuable assistance provided by G. Rakowsky

and the staff of the National Bureau of Standards' SURF II facility. This work was supported, in part, by the Office of Naval Research, the U.S. Department of Energy and NATO Grant No. 1939.

## REFERENCES

- 1 T.N. Rescigno, B.V. McKoy and B. Schneider, (Eds.), *Electron—Molecule and Photon—Molecule Collisions*, Plenum Press, New York, 1979.
- 2 V. Schmidt, *Appl. Opt.*, 19 (1980) 4080.
- 3 J.L. Dehmer, D. Dill and A.C. Parr, in S. McGlynn, G. Findley and R. Huebner (Eds.), *Photophysics and Photochemistry in the Vacuum Ultraviolet*, D. Reidel, Dordrecht, 1984, in press.
- 4 J.B. West, A.C. Parr, B.E. Cole, D.L. Ederer, R. Stockbauer and J.L. Dehmer, *J. Phys. B.*, 13 (1980) L105.
- 5 T.A. Carlson, M.O. Krause, D. Mehaffy, J.W. Taylor, F.A. Grimm and J.D. Allen, *J. Chem. Phys.*, 73 (1980) 6056.
- 6 S. Krummacher, V. Schmidt and F. Wuilleumier, *J. Phys. B.*, 13 (1980) 3993.
- 7 J.W. Davenport, *Phys. Rev. Lett.*, 36 (1976) 945.
- 8 J.L. Dehmer, D. Dill and S. Wallace, *Phys. Rev. Lett.*, 43 (1979) 1005.
- 9 D.M.P. Holland, A.C. Parr, D.L. Ederer, J.B. West and J.L. Dehmer, *Int. J. Mass Spectrom. Ion Phys.*, 52 (1983) 195.
- 10 D.M.P. Holland, A.C. Parr and J.L. Dehmer, *J. Phys. B.*, in press.
- 11 D.M. Rider, G.W. Ray, E.J. Darland and G.E. Leroi, *J. Chem. Phys.*, 74 (1981) 1652.
- 12 K. Watanabe, T. Nakayama and J. Mottl, *J. Quant. Spectrosc. Radiat. Transfer*, 2 (1962) 369.
- 13 A.J.C. Nicholson, *J. Chem. Phys.*, 43 (1965) 1171.
- 14 V.H. Dibeler and S.K. Liston, *J. Chem. Phys.*, 48 (1968) 4765.
- 15 R.S. Stradling and A.G. Loudon, *J. Chem. Soc. Faraday Trans. 2*, 73 (1977) 623.
- 16 C. Fridh, *J. Chem. Soc. Faraday Trans. 2*, 74 (1978) 2193.
- 17 D.C. Frost, F.G. Herring, C.A. McDowell and I.A. Stenhouse, *Chem. Phys. Lett.*, 4 (1970) 533.
- 18 R.F. Lake and H. Thompson, *Proc. R. Soc. London, Ser. A*, 317 (1970) 187.
- 19 D.W. Turner, C. Baker, A.D. Baker and C.R. Brundle, *Molecular Photoelectron Spectroscopy*, Wiley-Interscience, London, 1970, p. 345.
- 20 K. Kimura, S. Katsumata, Y. Achiba, T. Yamazaki and S. Iwata, *Handbook of Hel Photoelectron Spectra of Fundamental Organic Molecules*, Halstead Press, New York, 1981, p. 178.
- 21 L. Åsbrink, W. Von Niessen and G. Bieri, *J. Electron Spectrosc. Relat. Phenom.*, 21 (1980) 93.
- 22 T. Fujikawa, T. Ohta and H. Kuroda, *Chem. Phys. Lett.*, 28 (1974) 433.
- 23 T. Fujikawa, T. Ohta and H. Kuroda, *Bull. Chem. Soc. Jpn.*, 49 (1976) 1486.
- 24 T. Ha, *J. Mol. Struct.*, 11 (1972) 185.
- 25 P. Bayburt, M.F. Guest and I.H. Hillier, *Mol. Phys.*, 25 (1973) 1025.
- 26 G. Bieri, E. Heilbronner, V. Hornung, E. Kloster-Jensen, J.P. Maier, F. Thommen and W. Von Niessen, *Chem. Phys.*, 36 (1979) 1.
- 27 G.E. Leroi, private communication. Owing to a misassignment of the molecular orbitals in the original publication [11], the identifications used here have been altered.
- 28 A.C. Parr, R. Stockbauer, B.E. Cole, D.L. Ederer, J.L. Dehmer and J.B. West, *Nucl. Instrum. Methods*, 172 (1980) 357.
- 29 D.L. Ederer, B.E. Cole and J.B. West, *Nucl. Instrum. Methods*, 172 (1980) 185.
- 30 A.C. Parr, D.L. Ederer, J.B. West, D.M.P. Holland and J.L. Dehmer, *J. Chem. Phys.*, 76 (1982) 4349.